Exploring the bonding of large hydrocarbons on noble metals: Diindoperylene on Cu(111), Ag(111), and Au(111)

C. Bürker,[1] N. Ferri,[2] A. Tkatchenko,[2] A. Gerlach,[1] J. Niederhausen,[3] T. Hosokai,[1,4] S. Duhm,[5,6]
J. Zegenhagen,[7] N. Koch,[3] and F. Schreiber[1,*]

[1]*Institut für Angewandte Physik, Universität Tübingen, Auf der Morgenstelle 10, 72076 Tübingen, Germany*
[2]*Fritz-Haber-Institut der Max-Planck-Gesellschaft, Faradayweg 4-6, 14195 Berlin, Germany*
[3]*Institut für Physik, Humboldt-Universität zu Berlin, Newtonstrasse 15, 12489 Berlin, Germany*
[4]*Department of Materials Science and Engineering, Iwate University, Ueda 4-3-5, Morioka 020-8551, Japan*
[5]*Graduate School of Advanced Integration Science, Chiba University, Chiba 263-8522, Japan*
[6]*Institute of Functional Nano & Soft Materials (FUNSOM), Soochow University, 199 Ren-Ai Road, Suzhou 215123,
People's Republic of China*
[7]*European Synchrotron Radiation Facility, 6 Rue Jules Horowitz, Boîte Postale 220, 38043 Grenoble Cedex 9, France*

We present a benchmark study for the adsorption of a large π-conjugated organic molecule on different noble metal surfaces, which is based on x-ray standing wave (XSW) measurements and density functional theory calculations with van der Waals (vdW) interactions. The bonding distances of diindenoperylene on Cu(111), Ag(111), and Au(111) surfaces (2.51, 3.01, and 3.10 Å, respectively) determined with the normal-incidence XSW technique are compared with calculations. Excellent agreement with the experimental data, i.e., deviations less than 0.1 Å, is achieved using the Perdew-Burke-Ernzerhof (PBE) functional with vdW interactions that include the collective response of substrate electrons (the PBE + vdW^{surf} method). It is noteworthy that the calculations show that the vdW contribution to the adsorption energy increases in the order Au(111) < Ag(111) < Cu(111).

I. INTRODUCTION

The reliable prediction of the equilibrium structure and energetics of hybrid inorganic/organic systems from first principles represents a great challenge for theoretical methods due to the interplay of covalent interactions, electron transfer processes, Pauli repulsion, and van der Waals (vdW) interactions. During recent years, huge efforts have been made to incorporate vdW interactions into density functional theory (DFT) calculations in order to determine the structure and stability of π-conjugated organic molecules on solid surfaces.[1–6] Understanding these interface properties is relevant, *inter alia*, for electron transfer processes in organic devices. Until now and despite the obvious benefit, there are only a few studies of metal-organic interfaces combining theory and experiment. Here, x-ray standing wave (XSW) measurements can provide an important test for DFT calculations.[2,7] This is particularly important for systems with strong vdW contributions to the overall bonding, for which no simple substrate dependence is expected.

As model system we chose diindenoperylene (DIP, $C_{32}H_{16}$), a π-conjugated organic semiconductor with excellent optoelectronic device performance, which has been studied over the last decade both in thin films[8–11] and in monolayers on noble metal surfaces.[12–14] With respect to its chemical structure, DIP is a relatively simple, planar hydrocarbon without heteroatoms. In contrast to the intensely studied perylene derivative[15–20] 3,4,9,10-perylene tetracarboxylic dianhydrid (PTCDA, $C_{32}H_8O_6$) with its four keto groups, the DIP-substrate interaction is not complicated by polar side groups, and the influence of intermolecular interactions is expected to be smaller than for PTCDA.[21] Here, we present a systematic study with high-precision experimental data and state-of-the-art calculations of DIP adsorbed on Cu(111),

Ag(111), and Au(111). This allows us to assess the role and relative contribution of the vdW interactions, which, contrary to simplistic pictures, we find here to be lowest for the most polarizable substrate.

II. COMPUTATIONAL APPROACH

DFT calculations were performed using a method that extends standard pairwise vdW approaches[22,23] to model adsorbates on surfaces.[7] This was achieved by combining the DFT + vdW scheme[22] with the Lifshitz-Zaremba-Kohn (LZK) theory for vdW interactions between an atom and the surface[24,25] of a solid. In our approach (DFT + vdW^{surf}), the vdW energy is given by a sum of $C_6^{ab} R_{ab}^{-6}$ terms, where R_{ab} are the distances between atoms a and b, in analogy to standard pairwise dispersion corrected DFT methods. However, by employing the LZK theory we include the many-body collective response (*screening*) of the substrate electrons in the determination of the C_6 coefficients and vdW radii, going effectively beyond the pairwise description. Interface polarization effects are accounted for via the inclusion of semilocal hybridization due to the dependence of the C_6^{ab} interatomic coefficients on the electron density in the DFT + vdW method. The DFT + vdW^{surf} method has been shown to yield remarkably accurate results for the structure and adsorption energies of xenon, benzene, and PTCDA on a variety of (111) metal surfaces.[7,26] The FHI-AIMS code[27] was employed for our DFT calculations. The repeated-slab method was used to model all systems with the vacuum gap set to 20 Å. In all calculations, convergence criteria of 10^{-5} electrons for the electron density and 10^{-6} eV for the total energy of the system were used. A convergence criterion of 0.01 eV/Å for the maximum final force was

used for all structure relaxations. The scaled zeroth-order regular approximation (ZORA) was applied for inclusion of scalar relativistic effects.[28] The DFT + vdW^{surf} method employed the Perdew-Burke-Ernzerhof (PBE) functional.[29] The sampling of the Brillouin zone was done using a $(2 \times 2 \times 1)$ k-point grid.

We used a (7×7) unit cell composed of a metal surface of three layers and one single DIP molecule. In the absence of experimental data for the in-plane registry we placed the central ring of the molecule aligned with a topmost-metal-layer atom and the major axis of the molecule aligned along the cell diagonal. This structure was adopted for the Cu(111), Ag(111), and Au(111) surfaces. In each simulation we obtained the adsorption energy curve using a rigid DIP molecule and tuning the surface-molecule distance d. The adsorption energy per molecule E_{ads} was calculated from $E_{ads} = E_{tot} - (E_{surf} + E_{DIP})$, where E_{surf} is the energy per unit cell of the isolated metal surface, E_{DIP} is the energy per unit cell of the isolated DIP molecule, and E_{tot} is the energy per unit cell of the combined system. We also obtained the relaxed geometries for all three systems starting from the static equilibrium geometry. During geometry relaxation, we allowed only the topmost metal layer and the molecule to relax while the other two metal layers were fixed. From the final relaxed configurations we obtained the bonding distance d by taking the average position of all DIP carbon atoms with respect to the unrelaxed topmost surface layer. This definition is consistent with the analysis of the XSW data.

III. EXPERIMENTAL DETAILS

To measure the bonding distance of DIP we used the XSW technique,[30] which yields precise and element-specific structural data. The experiments were performed at beamline ID32 of the ESRF.[31] DIP films were prepared and studied *in situ* under ultrahigh-vacuum conditions. A separate preparation chamber contained a Knudsen cell, a quartz crystal microbalance, installations for Ar$^+$ sputtering, and a temperature-controlled sample stage. The main chamber, in which the XSW measurements were performed, was equipped with a sample manipulator and a hemispherical SPECS PHOIBOS 225 HV photoelectron analyzer. The XSW experiments were carried out at room temperature in back-reflection geometry using the (111) Bragg reflection of the crystals for at least two films per substrate to check for reproducibility of the results. The detection angle of the analyzer was $\sim 90°$ relative to the surface normal with an acceptance angle of $\pm 7.5°$. We note that in this configuration nondipolar contributions to the photoelecton yield can be effectively avoided.[32] The Cu(111), Ag(111), and Au(111) single crystals were mounted on different sample holders for individual treatment. The surfaces were prepared by repeated cycles of Ar$^+$ bombardment and annealing at 700 K. Surface cleanliness was confirmed with x-ray photoelectron spectroscopy (XPS) as well as low-energy electron diffraction (LEED). Sublimation-grade DIP was evaporated from a home-built Knudsen cell. The intensity ratio of the C 1s signal relative to a substrate core-level, normalized with the corresponding photoemission cross sections, was used to determine the number of DIP molecules on the surface. With the unit cell size
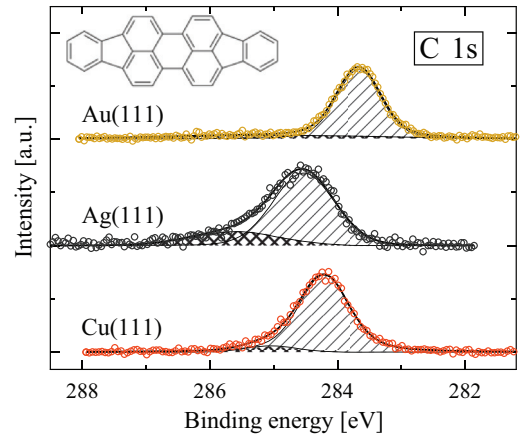

FIG. 1. (Color online) C 1s core-level shift observed for a submonolayer of DIP (inset) on Cu(111), Ag(111), and Au(111). The spectra were taken at an emission angle of 45° with the XSW setup at ID32. From each signal a Shirley background was subtracted and then it was fitted with a Voigt function for the main peak and a Gaussian function for possible shake-up peaks.

of DIP on Cu(111),[12] Ag(111),[13] and Au(111),[14] the coverages were calculated to be between 0.3 and 0.9 ML.

IV. RESULTS AND ANALYSIS

A. Experimental results

The C 1s core-level signals of DIP on Cu(111), Ag(111), and Au(111), which were used for the XSW measurements, are shown in Fig. 1. The main peaks are expected to consist of two principal components (C–C vs C–H bound atoms) which, however, could not be resolved with the energy resolution of the XSW setup. In addition to each main peak, a second weak feature at ~ 1 eV higher binding energy possibly related to a shake-up process can be observed. Obviously, the binding energy of the C 1s main line of DIP follows $E_B^{Ag} > E_B^{Cu} > E_B^{Au}$, being 284.5 eV on Ag(111), 284.2 eV on Cu(111), and 283.7 eV on Au(111). Furthermore, the C 1s peak of DIP on Ag(111) exhibits a stronger asymmetry than on Cu(111) and Au(111).[33] A detailed discussion of the spectroscopic features is beyond the scope of this paper, in which we focus on the XSW results.

Representative results of the XSW experiments are shown in Fig. 2(a). In each panel the measured reflectivity of the substrate and the corresponding C 1s photoelectron yield is displayed. Least-squares fits of the data give the coherent position P_H and hence the average bonding distance $d_H = d_0(1 + P_H)$,[36] where d_0 is the substrate lattice plane spacing. Based on results of all XSW experiments we calculate the average bonding distance d_H and the standard deviation; see Fig. 2(b). For Cu(111) we thus find (2.51 ± 0.03) Å, and for Ag(111) (3.01 ± 0.04) Å. Due to the reconstruction of the Au(111) surface, which results in a 3% larger spacing between the first and second Au layers,[17] the bonding distance decreases from the measured apparent value (3.17 ± 0.03) Å to (3.10 ± 0.03) Å. All experimental results are summarized in Table I.
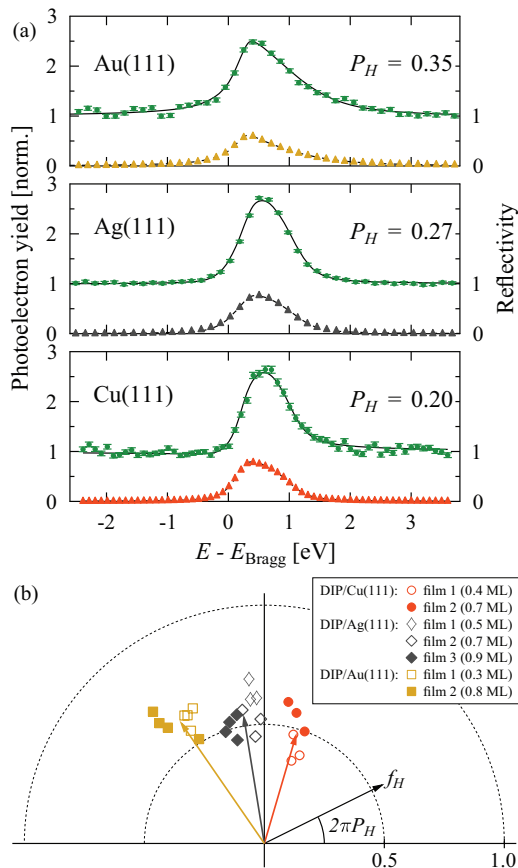
FIG. 2. (Color online) (a) Typical XSW data for DIP showing the reflectivity (triangles) and photoelectron yield (circles) of the C $1s$ signal on Cu(111), Ag(111), and Au(111). The solid lines correspond to least-squares fits of the reflectivity and photoelectron yield, which reveal the coherent position P_H and coherent fraction f_H. Bragg energies are $E_{Bragg} = 2.97$ keV [Cu(111)] and $E_{Bragg} = 2.63$ keV [Ag(111) and Au(111)]. (b) All XSW results for DIP on Cu(111), Ag(111), and Au(111) displayed in an Argand diagram. Here, each data point represents one single XSW measurement yielding f_H (length of a vector) and P_H (angle of a vector). The three vectors point to the average values of f_H and P_H for DIP on Cu(111), Ag(111), and Au(111). Film 1 of DIP on Ag(111) was measured with a different crystal compared to films 2 and 3.

Note that although the coverage of the two (three) DIP films prepared on each substrate was not identical, we did not observe a significantly coverage-dependent bonding distance d_H.

TABLE I. Results of XSW experiments: Coherent fraction f_H, coherent position P_H, and bonding distance d_H of DIP on the three noble metals. The parameters refer to an average of several XSW measurements with the corresponding standard deviation as error bars.

	f_H	P_H	d_H
Cu(111)	0.48 ± 0.09	0.20 ± 0.01	(2.51 ± 0.03) Å
Ag(111)	0.55 ± 0.08	0.28 ± 0.02	(3.01 ± 0.04) Å
Au(111)	0.62 ± 0.06	0.35 ± 0.01	(3.17 ± 0.03) Å[a]

[a]By taking the surface reconstruction of Au(111) into account, d_H is reduced to 3.10 Å.

TABLE II. Adsorption energy E_{ads} of the relaxed structures, vdW^{surf} binding energy E_{vdW} in parentheses as derived from data shown in Fig. 3, and distances d between the topmost layer of the metal and the carbon backbone of DIP. $d_{min/max}$ refer to the lowest/highest bonding distances of a carbon atom within a DIP molecule.

	E_{ads} (E_{vdW})	d	d_{min}	d_{max}
Cu(111)	-4.74 (-5.28) eV	2.59 Å	2.38 Å	2.79 Å
Ag(111)	-3.55 (-4.56) eV	2.94 Å	2.89 Å	3.01 Å
Au(111)	-2.53 (-3.06) eV	3.22 Å	3.15 Å	3.29 Å

Comparing these results with the bonding distances of PTCDA on the same metal surfaces, i.e., $d_H = 2.66$ Å on Cu(111),[16] $d_H = 2.86$ Å on Ag(111),[15,16] and $d_H = 3.27$ Å on Au(111),[17] we see that the bonding distances follow the same order, i.e., d_H(Cu) $< d_H$(Ag) $< d_H$(Au). Moreover, the results demonstrate that the absence of the C = O groups in DIP affects the bonding distance of the molecule only weakly.

B. Computational results

Having established precise experimental data, we now turn to the results of our DFT calculations. The average bonding distances of DIP obtained from fully relaxed structures are $d = 2.59$ Å on Cu(111), $d = 2.94$ Å on Ag(111), and $d = 3.22$ Å on Au(111), see Table II and Fig. 3. We hence find that the PBE + vdW^{surf} method applied to DIP on Cu(111), Ag(111), and Au(111) yields an agreement better than 0.1 Å between theoretical calculations and experiments. In accordance with the bonding distances, the calculated adsorption energies listed in Table II follow the trend $|E_{ads}(Cu)| > |E_{ads}(Ag)| > |E_{ads}(Au)|$. Interestingly, Fig. 3 shows that on Cu(111) the Pauli repulsion sets in rather weakly [a less steep $E_{ads}(d)$ for small distances] compared to Ag(111) and Au(111), which
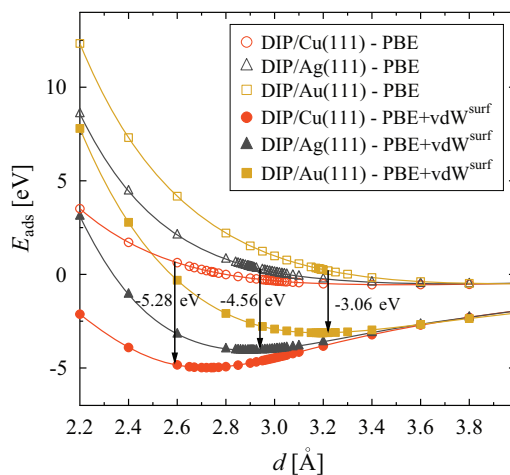

FIG. 3. (Color online) Adsorption energy E_{ads} for the unrelaxed DIP molecule as a function of its averaged distance d from the Cu(111), Ag(111), and Au(111) surfaces. The curves are shown for the PBE functional with and without the inclusion of long-range vdW interactions using the vdW^{surf} method. The reported contribution of the vdW energy is shown at the equilibrium distance corresponding to the fully relaxed DIP-surface geometry (see text).

is due to significant interaction between DIP and Cu(111). One may speculate that the interaction mechanism includes hybridization between DIP and Cu states.

In addition to the adsorption energies and average bonding distances, Table II holds the minimal and maximal bonding distances $d_{\text{min/max}}$ of individual carbon atoms in DIP. These values indicate that the molecule adsorbs in a slightly tilted or distorted geometry. For Cu(111), where the effect is most pronounced, the calculated bonding distances d_{min} and d_{max} differ by ~ 0.4 Å, which is equivalent to a molecular tilt angle of $1.5°$. The corresponding spread of vertical positions of the carbon atoms leads to a reduced f_H in the XSW scans. Model simulations similar to those presented in Ref. 37 show that the DFT-derived adsorption geometry on Cu(111) results in a relatively small decrease of the coherent fraction ($\Delta f_H = -0.07$), which lies within the standard deviation of our XSW measurements.

To obtain a better understanding of the influence of lateral intermolecular interactions on the DIP adsorption geometry, we also computed the relaxed DIP geometry for different Cu(111), Ag(111), and Au(111) unit cells. For DIP on Cu(111), we increased the unit cell from (7×7) to (9×7) in order to reduce the molecule-molecule interactions. We studied various configurations, finding a flat relaxed geometry for each case considered. The bonding distance is slightly larger (2.64 Å) than for the calculation with the smaller unit cell. For DIP on Ag(111), we also considered a unit cell which was determined from a closed packed monolayer on Ag(111).[13] The relaxed geometry of the molecules in the monolayer is flat and the bonding distance $d = 2.99$ Å in almost perfect agreement with the experimental one, i.e., even better than the result for Ag(111) shown in Table II. For a (9×5) unit cell of Au(111), the relaxed DIP geometry yields an equilibrium distance of 3.15 Å, also in slightly better agreement with experiment than the result shown in Table II. Overall, these calculations agree with the experimental observation that the vertical DIP position depends only weakly on surface coverage.

V. DISCUSSION

With the experimental and theoretical values at hand, and in view of their excellent agreement, we are in a good position to discuss the vdW interactions and the bonding distances in more detail. As described above, the (atom-atom) vdW energy is computed as $C_6^{ab} R_{ab}^{-6}$, where the C_6^{ab} coefficient determines the strength of the interaction between atoms a and b, while R_{ab} is the distance between adsorbate and substrate atoms (Fig. 3). Integration of the vdW energy for a single atom adsorbed on a semi-infinite surface yields the atom-surface vdW energy as[38,39] $C_3^{\text{A-S}}(z - z_0)^{-3}$, where now $C_3^{\text{A-S}}$ determines the interaction strength between atom and surface, z corresponds to the distance of the atom to the uppermost surface layer, and z_0 indicates the position of the surface image plane. In a rather naive picture, the $C_3^{\text{A-S}}$ coefficient can be determined simply from the C_6^{aa} and the C_6^{bb} coefficients that correspond to the adsorbed atom and the metal atom, respectively. However, the situation for real surfaces is more complex because both localized and bulk metal electrons contribute to the $C_3^{\text{A-S}}$ coefficient in a nontrivial
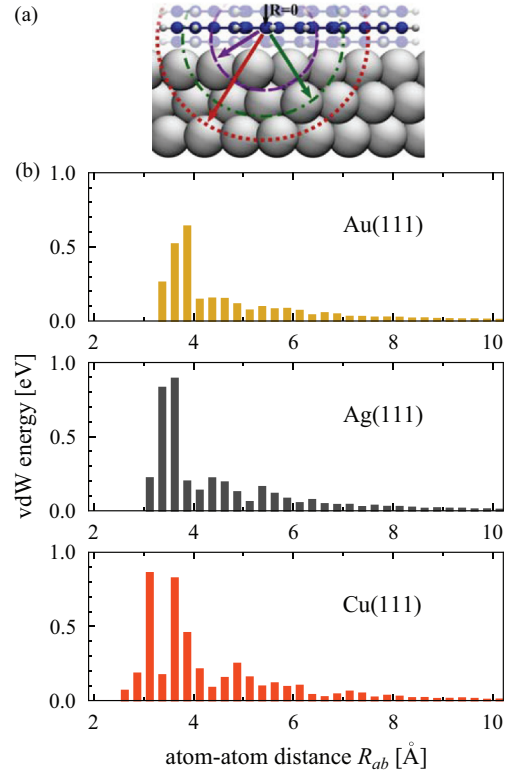

FIG. 4. (Color online) (a) Schematic picture of the adsorption of DIP on a (111) crystal. Each arrow corresponds to a certain distance R_{ab} between adsorbate and substrate atoms. (b) vdW energy of DIP adsorbed on Cu(111), Ag(111), and Au(111) as a function of the distance between adsorbate and substrate atoms.

way, meaning that this coefficient depends on the dielectric function of the underlying solid. We computed the $C_3^{\text{A-S}}$ coefficients corresponding to the interaction between a carbon atom and the Cu(111), Ag(111), and Au(111) surfaces. When describing the metal surface as a simple collection of noninteracting atoms we obtain $C_3^{\text{C-Cu}} = 0.68$, $C_3^{\text{C-Ag}} = 0.55$, and $C_3^{\text{C-Au}} = 0.50$ hartree bohr^3. In contrast, when using the more appropriate Lifshitz-Zaremba-Kohn expression[24,25] for $C_3^{\text{A-S}}$, we obtain $C_3^{\text{C-Cu}} = 0.35$, $C_3^{\text{C-Ag}} = 0.35$, and $C_3^{\text{C-Au}} = 0.33$ hartree bohr^3. This clearly illustrates that the vdW interaction between an atom and a solid surface is significantly modified by the collective electronic response within the substrate surface.[7,38,39] The very similar LZK C_3 coefficients for Cu, Ag, and Au lead to essentially the same adsorption energy at large distances for DIP on Cu(111), Ag(111), and Au(111) (Fig. 3). However, at shorter molecule-surface distances, which include the equilibrium distance, the adsorption energy is determined by an interplay between the vdW attraction and the Pauli repulsion, with a possible covalent component. The Pauli repulsion follows roughly the trend of decreasing vdW radii, with a faster onset in terms of the molecule-surface distance for Au (with the largest vdW radius), and then decreasing for Ag and Cu. Therefore, for Au the balance between the vdW attraction and the Pauli repulsion is obtained *further away* from the substrate (i.e., at larger adsorption distances) than for Cu, which in turn makes the adsorption energies *lower* for Au than for Cu, in contrast to the possible naive expectation of

Au with its higher polarizability and C_6 coefficient exhibiting a stronger vdW interaction than Cu.

The difference in the vdW energy distribution for DIP on Cu(111), Ag(111), and Au(111) is visualized in Fig. 4(b), where the vdW energy between DIP and substrate atoms is plotted as a function of their distance R_{ab}. In contrast to Ag(111) and Au(111), the small bonding distance of DIP on Cu(111) results in a second peak in the histogram at $\sim$3.6 Å, which originates from the higher atomic density of the Cu substrate.

VI. CONCLUSION

In conclusion, the bonding distances calculated with the PBE + vdW$^{\text{surf}}$ method are in excellent agreement with the XSW data for DIP on Cu(111), Ag(111), and Au(111)

(2.51, 3.01, and 3.10 Å, respectively). Our combined study demonstrates that the vdW energy is larger for DIP on Cu(111) than for DIP on Ag(111) and Au(111). Future investigations on the electronic properties of these systems, which can draw on the findings presented here, will contribute to an even better understanding of the adsorption process.

*Corresponding author: frank.schreiber@uni-tuebingen.de

[1] N. Atodiresei, V. Caciuc, P. Lazić, and S. Blügel, Phys. Rev. Lett. **102**, 136809 (2009).

[2] G. Mercurio, E. R. McNellis, I. Martin, S. Hagen, F. Leyssner, S. Soubatch, J. Meyer, M. Wolf, P. Tegeder, F. S. Tautz, and K. Reuter, Phys. Rev. Lett. **104**, 036102 (2010).

[3] D. Stradi, S. Barja, C. Díaz, M. Garnica, B. Borca, J. J. Hinarejos, D. Sánchez-Portal, M. Alcamí, A. Arnau, A. L. Vázquez de Parga, R. Miranda, and F. Martín, Phys. Rev. Lett. **106**, 186102 (2011).

[4] T. Olsen, J. Yan, J. J. Mortensen, and K. S. Thygesen, Phys. Rev. Lett. **107**, 156401 (2011).

[5] E. McNellis, Ph.D. thesis, Fritz-Haber-Institut der MPG, 2010.

[6] A. Tkatchenko, L. Romaner, O. T. Hofmann, E. Zojer, C. Ambrosch-Draxl, and M. Scheffler, MRS Bull. **35**, 435 (2010).

[7] V. G. Ruiz, W. Liu, E. Zojer, M. Scheffler, and A. Tkatchenko, Phys. Rev. Lett. **108**, 146103 (2012).

[8] A. C. Dürr, F. Schreiber, K. A. Ritley, V. Kruppa, J. Krug, H. Dosch, and B. Struth, Phys. Rev. Lett. **90**, 016104 (2003).

[9] S. Kowarik, A. Gerlach, S. Sellner, F. Schreiber, L. Cavalcanti, and O. Konovalov, Phys. Rev. Lett. **96**, 125504 (2006).

[10] U. Heinemeyer, K. Broch, A. Hinderhofer, M. Kytka, R. Scholz, A. Gerlach, and F. Schreiber, Phys. Rev. Lett. **104**, 257401 (2010).

[11] J. Wagner, M. Gruber, A. Hinderhofer, A. Wilke, B. Bröker, J. Frisch, P. Amsalem, A. Vollmer, A. Opitz, N. Koch, F. Schreiber, and W. Brütting, Adv. Funct. Mater. **20**, 4295 (2010).

[12] D. G. de Oteyza, E. Barrena, H. Dosch, and Y. Wakayama, Phys. Chem. Chem. Phys. **11**, 8741 (2009).

[13] H. Huang, J.-T. Sun, Y. P. Feng, W. Chen, and A. T. S. Wee, Phys. Chem. Chem. Phys. **13**, 20933 (2011).

[14] D. de Oteyza, E. Barrena, M. Ruiz-Oses, I. Silanes, B. Doyle, J. Ortega, A. Arnau, H. Dosch, and Y. Wakayama, J. Phys. Chem. C **112**, 7168 (2008).

[15] A. Hauschild, K. Karki, B. C. C. Cowie, M. Rohlfing, F. S. Tautz, and M. Sokolowski, Phys. Rev. Lett. **94**, 036106 (2005).

[16] A. Gerlach, S. Sellner, F. Schreiber, N. Koch, and J. Zegenhagen, Phys. Rev. B **75**, 045401 (2007).

[17] S. K. M. Henze, O. Bauer, T. L. Lee, M. Sokolowski, and F. S. Tautz, Surf. Sci. **601**, 1566 (2007).

[18] S. Duhm, A. Gerlach, I. Salzmann, B. Bröker, R. Johnson, F. Schreiber, and N. Koch, Org. Electron. **9**, 111 (2008).

[19] J. Ziroff, F. Forster, A. Schöll, P. Puschnig, and F. Reinert, Phys. Rev. Lett. **104**, 233004 (2010).

[20] P. Fenter, F. Schreiber, L. Zhou, P. Eisenberger, and S. R. Forrest, Phys. Rev. B **56**, 3046 (1997).

[21] L. Kilian, A. Hauschild, R. Temirov, S. Soubatch, A. Schöll, A. Bendounan, F. Reinert, T.-L. Lee, F. S. Tautz, M. Sokolowski, and E. Umbach, Phys. Rev. Lett. **100**, 136103 (2008).

[22] A. Tkatchenko and M. Scheffler, Phys. Rev. Lett. **102**, 073005 (2009).

[23] S. Grimme, J. Comput. Chem. **27**, 1787 (2006).

[24] E. M. Lifshitz, Sov. Phys. JETP **2**, 73 (1956).

[25] E. Zaremba and W. Kohn, Phys. Rev. B **13**, 2270 (1976).

[26] W. Liu, J. Carrasco, B. Santra, A. Michaelides, M. Scheffler, and A. Tkatchenko, Phys. Rev. B **86**, 245405 (2012).

[27] V. Blum, R. Gehrke, F. Hanke, P. Havu, V. Havu, X. Ren, K. Reuter, and M. Scheffler, Comput. Phys. Commun. **180**, 2175 (2009).

[28] E. van Lenthe, E. J. Baerends, and J. G. Snijders, J. Chem. Phys. **101**, 9783 (1994).

[29] J. P. Perdew, K. Burke, and M. Ernzerhof, Phys. Rev. Lett. **77**, 3865 (1996).

[30] D. P. Woodruff, Rep. Prog. Phys. **68**, 743 (2005).

[31] J. Zegenhagen, B. Detlefs, T.-L. Lee, S. Thiess, H. Isern, L. Petit, L. André, J. Roy, Y. Mi, and I. Joumard, J. Electron Spectrosc. Relat. Phenom. **178-179**, 258 (2010).

[32] F. Schreiber, K. A. Ritley, I. A. Vartanyants, H. Dosch, J. Zegenhagen, and B. C. C. Cowie, Surf. Sci. Lett. **486**, 519 (2001).

[33] This may be related to the creation of electron-hole pairs close to the Fermi level caused by the higher density of states near the Fermi edge of DIP adsorbed on Ag(111) (Refs. 34 and 35).

[34] S. Krause, Ph.D. thesis, Universität Würzburg, 2009.

[35] S. Krause, A. Schöll, and E. Umbach, Org. Electron. **14**, 584 (2013).

[36] J. Zegenhagen, Surf. Sci. Rep. **18**, 199 (1993).

[37] A. Gerlach, T. Hosokai, S. Duhm, S. Kera, O. T. Hofmann, E. Zojer, J. Zegenhagen, and F. Schreiber, Phys. Rev. Lett. **106**, 156102 (2011).

[38] L. W. Bruch, R. D. Diehl, and J. A. Venables, Rev. Mod. Phys. **79**, 1381 (2007).

[39] L. W. Bruch, M. W. Cole, and E. Zaremba, *Physical Adsorption: Forces and Phenomena* (Dover, New York, 2009).